Gluon multiplicity in coherent diffraction of onium on a heavy nucleus

Yang Li[1] and Kirill Tuchin[1,2]

[1]*Department of Physics and Astronomy, Iowa State University, Ames, Iowa 50011, USA*
[2]*RIKEN BNL Research Center, Upton, New York 11973-5000, USA*

(Received 26 February 2008; published 11 June 2008)

We derive the cross section for the diffractive gluon production in high energy onium-nucleus collisions that includes the low-x evolution effects in the rapidity interval between the onium and the produced gluon and in the rapidity interval between the gluon and the target nucleus. We analyze our result in two limiting cases: when the onium size is much smaller than the saturation scale and when its size is much larger than the saturation scale. In the later case the gluon multiplicity is very small in the quasiclassical case and increases when the low-x evolution effects in onium become significant. We discuss the implications of our result for the Relativistic Heavy Ion Collider, Large Hadron Collider, and Electron Ion Collider phenomenology.

DOI: 10.1103/PhysRevD.77.114012 PACS numbers: 13.60.Hb, 13.85.Hd

I. INTRODUCTION

Diffractive gluon production in high energy pA collisions and in deep inelastic scattering (DIS) is a sensitive probe of the color glass condensate [1–10] characterized by high parton density and gluon saturation [11,12]. Diffractive processes played a pivotal role in identifying the first signatures of the gluon saturation in DIS at HERA [13–21]. They are of great interest as a tool for studying the low-x dynamics in pA collisions at the Relativistic Heavy Ion Collider (RHIC) and the Large Hadron Collider (LHC) as well as in DIS at the proposed Electron Ion Collider (EIC). The study of high parton densities in deuteron–gold collisions at RHIC, has provided many novel insights into the structure of nuclear matter and has been focused on inclusive processes. By triggering on hadrons in the deuteron fragmentation region (''forward'' rapidity) one is able to access very low values of Bjorken x that are sensitive to the gluon saturation. Investigation of energy, rapidity, centrality, and transverse momentum dependence of various production channels offers an opportunity to attain a better understanding of the nuclear and hadron structure at low x. Among the channels which have been discussed in this context are total hadron multiplicities [22–25], inclusive production of gluons [26–35], heavy quarks [36–42], valence quarks [43,44], prompt photons [45], dileptons [46–48], and identified hadrons [49] (for a review, see, e.g., [50,51]). Diffractive production in pA collisions offers another avenue for exploring the low-x dynamics. Motivated by a possibility to measure the diffractive production in pA collisions at RHIC and LHC, we analyze in this paper diffractive gluon production in onium–heavy nucleus collisions. We intentionally avoid discussing the ''dipole content'' of the proton light-cone ''wave function'' and concentrate entirely on quantities that can be calculated in perturbation theory. Our results can be equally well applied to diffractive gluon production in DIS in which the light-cone ''wave function'' of the virtual photon is well-known. Diffractive gluon production in DIS has been discussed in many publications [14,52–59] and has been limited to the quasiclassical approximation and/or phenomenological models. In this paper we go beyond the quasiclassical approximation and include the low-x evolution effects at all rapidity intervals.

The paper is structured as follows. In Sec. II we review the result for diffractive gluon production in the quasiclassical approximation derived in [55,60,61]. In Sec. III we generalize these results by including the effect of quantum evolution. We consider separately the case when the rapidity gap Y_0 between the produced gluon and the target equals the gluon's rapidity y (Fig. 2) and a more general case when $y \geq Y_0$ (Fig. 3). The corresponding cross sections are given by (14) and (16) in terms of the dipole distribution in proton $n_p(\mathbf{r}, \mathbf{r}', \mathbf{b}, y)$, the forward dipole-nucleus scattering amplitude $N(\mathbf{r}, \mathbf{b}, y)$, and diffractive dipole-nucleus scattering amplitude $N_D(\mathbf{r}, \mathbf{b}, y; Y_0)$. In Sec. IV we review the main properties of $n_p(\mathbf{r}, \mathbf{r}', \mathbf{b}, y)$ and $N(\mathbf{r}, \mathbf{b}, y)$ in the linear regime and in the saturation regime and demarcate the kinematic landscape. We then proceed in Sec. V by performing analysis of the diffractive gluon production in the quasiclassical approximation in various kinematic regions. The results are displayed in (51) and (56). In Sec. VI we do similar analysis in the case of low-x evolution, see (62) and (65). We summarize and discuss the phenomenological importance of the obtained results in Sec. VII.

II. DIFFRACTIVE GLUON PRODUCTION IN THE QUASI-CLASSICAL APPROXIMATION

The quasiclassical approximation of the hadron-nucleus interactions is valid when a typical parton coherence length l_c is much larger than the nuclear size R_A in the nucleus rest frame. The former is approximately given by $l_c \approx \frac{1}{2m_N x}$, where m_N is a nucleon mass. It follows that the quasiclassical approximation holds for $x \lesssim \frac{1}{R_A m_N}$. Owing to the large

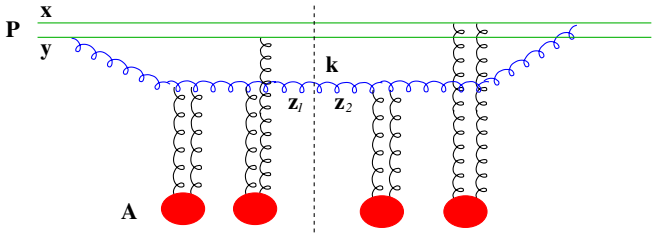

FIG. 1 (color online). One of the diagrams contributing to the diffractive gluon production in onium (P)—heavy nucleus (A) collisions in the quasiclassical approximation. Notations are explained in the text.

coherence length, the process of diffractive production can be considered as proceeding in two stages: gluon emission long time before the collision followed by the instantaneous interaction. This picture is particularly simple in the transverse configuration space since the parton transverse coordinates do not change in the course of instantaneous interaction. As the result, the cross section can be represented as a convolution of the proton's light-cone "wave function" and the scattering amplitude in the transverse configuration space, see Fig. 1. In the quasiclassical approximation, the cross section for the diffractive gluon production in onium-heavy nucleus collisions has been derived in [55,60,61]. Using notations of [55], see Fig. 1, it reads

$$\begin{aligned}\frac{d\sigma(k,y)}{d^2k\,dy} &= \frac{\alpha_s C_F}{\pi^2}\frac{1}{(2\pi)^2}\int d^2b\,d^2z_1\,d^2z_2\,e^{-i\mathbf{k}\cdot(\mathbf{z}_1-\mathbf{z}_2)} \\ &\times\left(\frac{\mathbf{z}_1-\mathbf{x}}{|\mathbf{z}_1-\mathbf{x}|^2}-\frac{\mathbf{z}_1-\mathbf{y}}{|\mathbf{z}_1-\mathbf{y}|^2}\right) \\ &\cdot\left(\frac{\mathbf{z}_2-\mathbf{x}}{|\mathbf{z}_2-\mathbf{x}|^2}-\frac{\mathbf{z}_2-\mathbf{y}}{|\mathbf{z}_2-\mathbf{y}|^2}\right) \\ &\times\left(e^{-P(\mathbf{x},\mathbf{y},\mathbf{z}_1)}-e^{-(C_F/4N_c)(\mathbf{x}-\mathbf{y})^2Q_{s0}^2}\right) \\ &\times\left(e^{-P(\mathbf{x},\mathbf{y},\mathbf{z}_2)}-e^{-(C_F/4N_c)(\mathbf{x}-\mathbf{y})^2Q_{s0}^2}\right), \end{aligned} \tag{1}$$

where $\mathbf{x}$ and $\mathbf{y}$ are the transverse coordinates of quark and antiquark, $\mathbf{z}_1$, $\mathbf{z}_2$ are the transverse coordinates of the gluon in the amplitude and the complex-conjugate amplitude correspondingly, see Fig. 1. The $q\bar{q}g$ propagator reads [37,61,62]

$$\begin{aligned}\exp\{-P(\mathbf{x},\mathbf{y},\mathbf{z})\} = \exp\Big(&-\frac{1}{8}(\mathbf{x}-\mathbf{z})^2Q_{s0}^2-\frac{1}{8}(\mathbf{y}-\mathbf{z})^2Q_{s0}^2 \\ &+\frac{1}{8N_c^2}(\mathbf{x}-\mathbf{y})^2Q_{s0}^2\Big).\end{aligned} \tag{2}$$

The *gluon* saturation scale is given by

$$Q_{s0}^2 = \frac{4\pi^2\alpha_s N_c}{N_c^2-1}\rho T(\mathbf{b})xG(x,1/\mathbf{r}^2), \tag{3}$$

where ρ is the nuclear density, $T(\mathbf{b})$ is the nuclear thickness function as a function of the impact parameter $\mathbf{b}$. The gluon distribution function reads

$$xG(x,1/\mathbf{r}^2) = \frac{\alpha_s C_F}{\pi}\ln\frac{1}{\mathbf{r}^2\Lambda^2}, \tag{4}$$

with Λ being some nonperturbative momentum scale characterizing the nucleon's wave function.

In the framework of the dipole model [63], the gluon evolution is easily accounted for in the large N_c approximation. Let us introduce the forward elastic dipole-nucleus scattering amplitude $N(\mathbf{r},\mathbf{b},Y)$. In the quasiclassical approximation it reads [64]

$$N(\mathbf{r},\mathbf{b},0) = 1-e^{-(1/8)\mathbf{r}^2Q_{s0}^2}. \tag{5}$$

At large N_c, (1), (2), and (5) yield

$$\begin{aligned}\frac{d\sigma(k,y)}{d^2k\,dy} = \frac{\alpha_s C_F}{\pi^2}\frac{1}{(2\pi)^2}\int d^2b\,d^2z_1\,d^2z_2\,e^{-i\mathbf{k}\cdot(\mathbf{z}_1-\mathbf{z}_2)}&\left(\frac{\mathbf{z}_1-\mathbf{x}}{|\mathbf{z}_1-\mathbf{x}|^2}-\frac{\mathbf{z}_1-\mathbf{y}}{|\mathbf{z}_1-\mathbf{y}|^2}\right)\cdot\left(\frac{\mathbf{z}_2-\mathbf{x}}{|\mathbf{z}_2-\mathbf{x}|^2}-\frac{\mathbf{z}_2-\mathbf{y}}{|\mathbf{z}_2-\mathbf{y}|^2}\right) \\ &\times[N(\mathbf{x}-\mathbf{y},\mathbf{b},0)-N(\mathbf{x}-\mathbf{z}_1,\mathbf{b},0)-N(\mathbf{y}-\mathbf{z}_1,\mathbf{b},0)+N(\mathbf{x}-\mathbf{z}_1,\mathbf{b},0)N(\mathbf{y}-\mathbf{z}_1,\mathbf{b},0)] \\ &\times[N(\mathbf{x}-\mathbf{y},\mathbf{b},0)-N(\mathbf{x}-\mathbf{z}_2,\mathbf{b},0)-N(\mathbf{y}-\mathbf{z}_2,\mathbf{b},0)+N(\mathbf{x}-\mathbf{z}_2,\mathbf{b},0)N(\mathbf{y}-\mathbf{z}_2,\mathbf{b},0)].\end{aligned} \tag{6}$$

Integrating (6) over all transverse momenta yields delta function $(2\pi)^2\delta(\mathbf{z}_1-\mathbf{z}_2)$. Hence, the total cross section per unit rapidity reads after a simple calculation

$$\frac{d\sigma(y)}{dy} = \frac{\alpha_s C_F}{\pi^2}\int d^2b\,d^2z\,\frac{(\mathbf{x}-\mathbf{y})^2}{(\mathbf{x}-\mathbf{z})^2(\mathbf{y}-\mathbf{z})^2}[N(\mathbf{x}-\mathbf{y},\mathbf{b},0)-N(\mathbf{x}-\mathbf{z},\mathbf{b},0)-N(\mathbf{y}-\mathbf{z},\mathbf{b},0)+N(\mathbf{x}-\mathbf{z},\mathbf{b},0)N(\mathbf{y}-\mathbf{z},\mathbf{b},0)]^2.$$

III. INCLUDING QUANTUM EVOLUTION

When the collision energy becomes high enough, multiple gluon emission becomes possible. Parametrically, each gluon emission brings in a factor $\alpha_s\ln(1/x)$. Accordingly, quantum evolution takes place when $x \lesssim e^{-(1/\alpha_s)}$. Let the incident onium be characterized by the two-vector $\mathbf{r}$. In the course of evolution, dipoles of different sizes are produced until

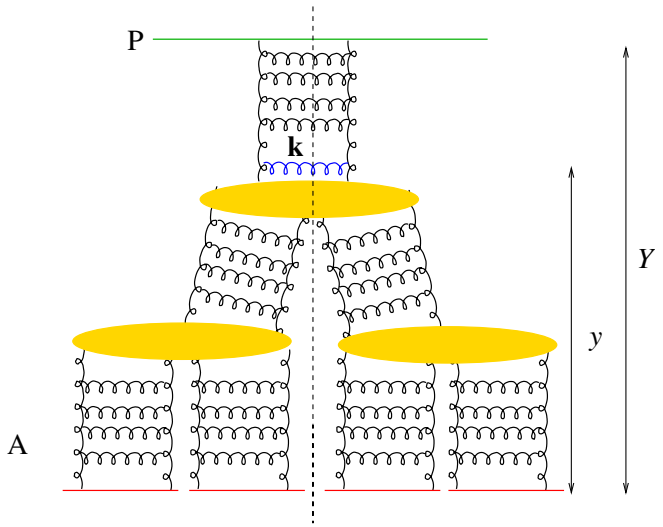

FIG. 2 (color online). Fan diagram describing the diffractive gluon production in onium (P)—heavy nucleus (A) collisions with the rapidity gap being equal to the rapidity of the produced gluon.

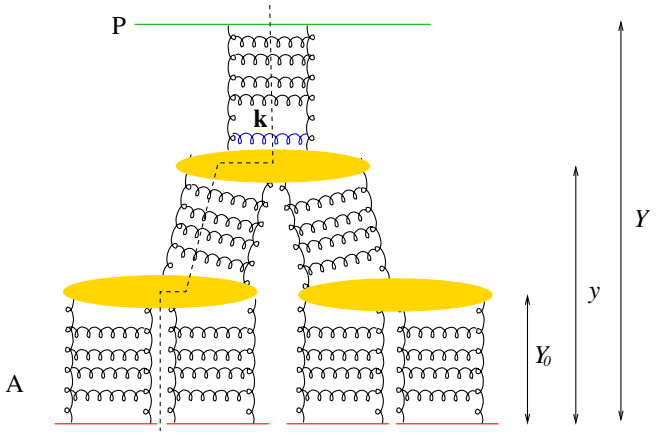

FIG. 3 (color online). Fan diagram for the diffractive gluon production in onium (P)—heavy nucleus (A) collisions with rapidity gap Y_0 smaller than the gluon rapidity y.

eventually a dipole of size $\mathbf{r}'$ emits a gluon at rapidity y with transverse momentum $\mathbf{k}$. In terms of the Regge theory, evolution in the rapidity interval between the original onium and the emitted gluon corresponds to exchange of a single Pomeron, in agreement with the Abramovsky-Gribov-Kancheli cutting rules [27,65]. Afterwards, i.e., in the rapidity interval between the emitted gluon and the target nucleus, evolution is nonlinear and corresponds to exchange of diffractively cut fan diagram, see Fig. 2 and 3. The general method for including the nonlinear low-x evolution into inclusive processes in the dipole model framework was derived in [27] and is applied later in this section.

We would like to separately consider the following two cases: (i) rapidity gap Y_0 equals the produced gluon rapidity y, see Fig. 2, and (ii) a more general case $Y_0 \leq y$, see Fig. 3. In later sections we will focus our attention on the former case. The reason is that experimentally, diffractive production is usually measured per unit of invariant mass of the diffractively produced system (rather than per dk^2). The invariant mass is given by $M^2 = k^2/x$ where $\mathbf{k}$ and $x = e^{-(Y-y)}$ refer to the slowest particle in the gluon cascade originating from proton. That being the case, it is sufficient to consider production of a gluon adjacent to the rapidity gap as depicted in Fig. 2. This case corresponds to the rapidity gap Y_0 being equal to the rapidity of the produced gluon $Y_0 = y$.

A. Gluon production with $y = Y_0$

The relevant fan diagram is displayed in Fig. 2. We include the evolution effects using the method derived in [27]. We obtain the following generalization of (6):

$$\frac{d\sigma(k,y)}{d^2k\,dy} = \frac{\alpha_s C_F}{\pi^2}\frac{1}{(2\pi)^2}\int d^2b\,d^2B \times \int d^2r' n_1(\mathbf{r},\mathbf{r}',\mathbf{B}-\mathbf{b},Y-y)|\mathbf{I}(\mathbf{r}',\mathbf{k},y)|^2, \tag{7}$$

where

$$\mathbf{I}(\mathbf{x}'-\mathbf{y}',\mathbf{k},y) = \int d^2z_1 e^{-i\mathbf{k}\cdot\mathbf{z}_1}\left(\frac{\mathbf{z}_1-\mathbf{x}'}{|\mathbf{z}_1-\mathbf{x}'|^2}-\frac{\mathbf{z}_1-\mathbf{y}'}{|\mathbf{z}_1-\mathbf{y}'|^2}\right)[N(\mathbf{x}'-\mathbf{y}',\mathbf{b},y)-N(\mathbf{x}'-\mathbf{z}_1,\mathbf{b},y)-N(\mathbf{y}'-\mathbf{z}_1,\mathbf{b},y) + N(\mathbf{x}'-\mathbf{z}_1,\mathbf{b},y)N(\mathbf{y}'-\mathbf{z}_1,\mathbf{b},y)]. \tag{8}$$

Here $n_1(\mathbf{x}-\mathbf{y},\mathbf{x}'-\mathbf{y}',\mathbf{B}-\mathbf{b},Y-y)$ has the meaning of the number of dipoles of size $\mathbf{x}'-\mathbf{y}'$ at rapidity $Y-y$ and impact parameter $\mathbf{b}$ generated by evolution from the original dipole $\mathbf{x}-\mathbf{y}$ having rapidity Y and impact parameter $\mathbf{B}$ [63]. It satisfies the Balitsky-Fadin-Kuraev-Lipatov (BFKL) equation [66,67]

$$\frac{\partial n_1(\mathbf{x}-\mathbf{y},\mathbf{x}'-\mathbf{y}',\mathbf{b},y)}{\partial y} = \frac{\alpha_s N_c}{2\pi^2}\int d^2z\frac{(\mathbf{x}-\mathbf{y})^2}{(\mathbf{x}-\mathbf{z})^2(\mathbf{y}-\mathbf{z})^2}[n_1(\mathbf{x}-\mathbf{z},\mathbf{x}'-\mathbf{y}',\mathbf{b},y)+n_1(\mathbf{y}-\mathbf{z},\mathbf{x}'-\mathbf{y}',\mathbf{b},y) - n_1(\mathbf{x}-\mathbf{y},\mathbf{x}'-\mathbf{y}',\mathbf{b},y)], \tag{9}$$

with the initial condition

$$n_1(\mathbf{r}, \mathbf{r}', \mathbf{b}, 0) = \delta(\mathbf{r} - \mathbf{r}')\delta(\mathbf{b}), \tag{10}$$

where we denoted $\mathbf{r} = \mathbf{x} - \mathbf{y}$ and $\mathbf{r}' = \mathbf{x}' - \mathbf{y}'$.

The forward elastic dipole-nucleus scattering amplitude satisfies the nonlinear Balitsky-Kovchegov (BK) equation [68,69]

$$\frac{\partial N(\mathbf{x} - \mathbf{y}, \mathbf{b}, y)}{\partial y} = \frac{\alpha_s N_c}{2\pi^2} \int d^2z \frac{(\mathbf{x} - \mathbf{y})^2}{(\mathbf{x} - \mathbf{z})^2(\mathbf{y} - \mathbf{z})^2} \times [N(\mathbf{x} - \mathbf{z}, \mathbf{b}, y) + N(\mathbf{y} - \mathbf{z}, \mathbf{b}, y) - N(\mathbf{x} - \mathbf{y}, \mathbf{b}, y) - N(\mathbf{x} - \mathbf{z}, \mathbf{b}, y) \times N(\mathbf{y} - \mathbf{z}, \mathbf{b}, y)], \tag{11}$$

with the initial condition given by (5). In writing both Eqs. (9) and (11), we assumed that the absolute value of impact parameter $\mathbf{b}$ is much larger than the typical dipole size. This is a justified approximation for a scattering off a heavy nucleus.

In order to keep expressions as compact as possible, it is convenient to assume that the nuclear profile is cylindrical. This simple model allows correct identification of the atomic number (i.e., centrality) dependence of the cross sections. An explicit impact parameter dependence, which is required for numerical analysis, can be easily restored in the final expressions. Since we are not concerned here with the details of the impact parameter dependence, we integrate (9) over $\underline{b}$. The quantity

$$n_p(\mathbf{r}, \mathbf{r}', y) = \int d^2b n_1(\mathbf{r}, \mathbf{r}', \mathbf{b}, y) \tag{12}$$

in turn satisfies the BFKL equation with the initial condition

$$n_p(\mathbf{r}, \mathbf{r}', 0) = \delta(\mathbf{r} - \mathbf{r}'). \tag{13}$$

In terms of $n_p(\mathbf{r}, \mathbf{r}', y)$, (7) reads

$$\frac{d\sigma(k, y)}{d^2k dy} = \frac{\alpha_s C_F}{\pi^2} \frac{1}{(2\pi)^2} S_A \int d^2r' n_p(\mathbf{r}, \mathbf{r}', Y - y) \times |\mathbf{I}(\mathbf{r}', \mathbf{k}, y)|^2, \tag{14}$$

where S_A is the cross sectional area of the interaction region.

The total cross section for diffractive gluon production is convenient to write in the following form:

$$\frac{d\sigma(y)}{dy} = \frac{\alpha_s C_F}{\pi^2} S_A \int d^2\mathbf{r}' n_p(\mathbf{r}, \mathbf{r}', Y - y) \times \int d^2w \frac{\mathbf{r}'^2}{(\mathbf{w} - \mathbf{r}')^2\mathbf{w}^2} [N(\mathbf{r}', \mathbf{b}, y) - N(\mathbf{w} - \mathbf{r}', \mathbf{b}, y) - N(\mathbf{w}, \mathbf{b}, y) + N(\mathbf{w} - \mathbf{r}', \mathbf{b}, y)N(\mathbf{w}, \mathbf{b}, y)]^2, \tag{15}$$

where we introduced a new variable $\mathbf{w} = \mathbf{z} - \mathbf{y}'$ such that w is the size of one of the daughter dipoles formed by emission of a gluon at point $\mathbf{z}$ by a parent dipole $\mathbf{r}' = \mathbf{x}' - \mathbf{y}'$.

B. Diffractive production with $Y_0 < y$

So far we have been concentrating on a case in which the rapidity of the produced gluon y coincides with the rapidity gap Y_0 in a diffractive event. In this case, the diffractive scattering amplitude $N_D(\mathbf{r}, \mathbf{b}, y, Y_0)$ coincides with the square of the forward elastic scattering amplitude $N(\mathbf{r}, \mathbf{b}, y)$. In principle, a question may arise about the diffractive production of a gluon with $y > Y_0$. Such process is shown in Fig. 3. For the processes in which the transverse coordinate of the gluon in the amplitude $\mathbf{z}_1$ is approximately the same as the its coordinate in the c.c amplitude $\mathbf{z}_2$, the corresponding cross section is still given by (14)

$$\frac{d\sigma(k, y)}{d^2k dy} = \frac{\alpha_s C_F}{\pi^2} \frac{1}{(2\pi)^2} S_A \int d^2r' n_p(\mathbf{r}, \mathbf{r}', Y - y) \times |\mathbf{I}(\mathbf{r}', \mathbf{k}, y; Y_0)|^2, \tag{16}$$

where now in place of (8) we write

$$\mathbf{I}(\mathbf{x}' - \mathbf{y}', \mathbf{k}, y; Y_0) = \int d^2z_1 e^{-i\mathbf{k}\cdot\mathbf{z}_1} \left(\frac{\mathbf{z}_1 - \mathbf{x}'}{|\mathbf{z}_1 - \mathbf{x}'|^2} - \frac{\mathbf{z}_1 - \mathbf{y}'}{|\mathbf{z}_1 - \mathbf{y}'|^2} \right) [N_D^{(1/2)}(\mathbf{x}' - \mathbf{y}', \mathbf{b}, y; Y_0) - N_D^{1/2}(\mathbf{x}' - \mathbf{z}_1, \mathbf{b}, y; Y_0) - N_D^{1/2}(\mathbf{y}' - \mathbf{z}_1, \mathbf{b}, y; Y_0) + N_D^{1/2}(\mathbf{x}' - \mathbf{z}_1, \mathbf{b}, y; Y_0) N_D^{1/2}(\mathbf{y}' - \mathbf{z}_1, \mathbf{b}, y; Y_0)]. \tag{17}$$

The amplitude $N_D(\mathbf{r}, \mathbf{b}, y; Y_0)$ equals to the cross section of single diffractive dissociation of a dipole of transverse size $\mathbf{r}$, rapidity y, and impact parameter $\mathbf{b}$ on a target nucleus. It satisfies the Kovchegov–Levin evolution equation [70]

$$\frac{\partial N_D(\mathbf{x} - \mathbf{y}, \mathbf{b}, y; Y_0)}{\partial y} = \frac{2\alpha_s C_F}{\pi^2} \int d^2z \left[\frac{(\mathbf{x} - \mathbf{y})^2}{(\mathbf{x} - \mathbf{z})^2(\mathbf{y} - \mathbf{z})^2} - 2\pi\delta(\mathbf{y} - \mathbf{z}) \ln(|\mathbf{x} - \mathbf{y}|\Lambda) \right] N_D(\mathbf{x} - \mathbf{z}, \mathbf{b}, y; Y_0) + \frac{\alpha_s C_F}{\pi^2} \int d^2z \frac{(\mathbf{x} - \mathbf{y})^2}{(\mathbf{x} - \mathbf{z})^2(\mathbf{y} - \mathbf{z})^2} [N_D(\mathbf{x} - \mathbf{z}, \mathbf{b}, y; Y_0) N_D(\mathbf{y} - \mathbf{z}, \mathbf{b}, y; Y_0) - 4N_D(\mathbf{x} - \mathbf{z}, \mathbf{b}, y; Y_0) N(\mathbf{y} - \mathbf{z}, \mathbf{b}, y) + 2N(\mathbf{x} - \mathbf{z}, \mathbf{b}, y) N(\mathbf{y} - \mathbf{z}, \mathbf{b}, y)], \tag{18}$$

with the initial condition

$$N_D(\mathbf{r}, \mathbf{b}, y = Y_0; Y_0) = N^2(\mathbf{r}, \mathbf{b}, Y_0). \tag{19}$$

Diffractive gluon production of the kind shown in Fig. 3 requires a dedicated study and will certainly lead to a number of interesting observations. We are going to perform such analysis in future publications. In this paper we concentrate on the case $y = Y_0$.

IV. DIPOLE EVOLUTION IN ONIUM AND NUCLEUS

A. Dipole evolution in onium

Dipole evolution in onium is encoded in the function $n_1(\mathbf{r}, \mathbf{r}', \mathbf{b}, y)$ and is determined by solving Eq. (9) with the initial condition (10). In the case of a cylindrical profile we use function $n_p(\mathbf{r}, \mathbf{r}', y)$ instead. The general solution of the BFKL equation for $n_p(\mathbf{r}, \mathbf{r}', y)$ reads

$$n_p(\mathbf{r}, \mathbf{r}', y) = \int_{-\infty}^{\infty} d\nu e^{2\bar{\alpha}_s \chi(\nu) y} (r/r')^{1+2i\nu} C_\nu^p, \tag{20}$$

where $\bar{\alpha}_s = \alpha_s N_c/\pi$ and the leading BFKL eigenvalue

$$\chi(\nu) = \psi(1) - \tfrac{1}{2}\psi\left(\tfrac{1}{2} - i\nu\right) - \tfrac{1}{2}\psi\left(\tfrac{1}{2} + i\nu\right), \tag{21}$$

with $\psi(\nu)$ being the digamma function

$$\psi(\nu) = \frac{\Gamma'(\nu)}{\Gamma(\nu)}. \tag{22}$$

The Mellin image C_ν^p can be found using the formula

$$\delta(\mathbf{r} - \mathbf{r}') = \frac{1}{2\pi^2 r'^2} \int_{-\infty}^{\infty} d\nu (r/r')^{1+2i\nu}. \tag{23}$$

The result is

$$n_p(\mathbf{r}, \mathbf{r}', y) = \frac{1}{2\pi^2 r'^2} \int_{-\infty}^{\infty} d\nu e^{2\bar{\alpha}_s \chi(\nu) y} (r/r')^{1+2i\nu}. \tag{24}$$

The integral over ν can be done analytically in two important limits. In the leading logarithmic approximation (LLA) we expand the function $\chi(\nu)$ near the minimum at $\nu = 0$ as

$$\chi(\nu)_{\mathrm{LLA}} \approx 2\ln 2 - 7\zeta(3)\nu^2, \tag{25}$$

where $\zeta(z)$ is the Riemann zeta function. Substituting (25) into (24) and integrating around the saddle point

$$\nu_p^\star = \frac{i \ln(r/r')}{14\zeta(3)\bar{\alpha}_s y}, \tag{26}$$

we derive

$$n_p(\mathbf{r}, \mathbf{r}', y)_{\mathrm{LLA}} \approx \frac{1}{2\pi^2 r r'} \sqrt{\frac{\pi}{14\zeta(3)\bar{\alpha}_s y}} \times e^{(\alpha_P - 1)y} e^{-(\ln^2(r'/r)/14\zeta(3)\bar{\alpha}_s y)}, \quad \alpha_s y \gg \ln^2(r/r'), \tag{27}$$

where $\alpha_P - 1 = 4\bar{\alpha}_s \ln 2$.

Alternatively, we can expand $\chi(\nu)$ near one of its two symmetric poles at $2i\nu = \pm 1$. This corresponds to the double-logarithmic approximation (DLA). The choice of a particular pole depends on the relation between r and r'. Expanding near $2i\nu = 1$ we attain

$$\chi(\nu)_{\mathrm{DLA}} \approx \frac{1}{1 - 2i\nu}. \tag{28}$$

Plugging this into (24) we have

$$n_p(\mathbf{r}, \mathbf{r}', y)_{\mathrm{DLA}} \approx \frac{1}{2\pi^2 r'^2} \int_{-\infty}^{\infty} d\nu e^{(2\bar{\alpha}_s y/1 - 2i\nu) + (1+2i\nu)\ln(r/r')}. \tag{29}$$

The saddle point of the expression in the exponent is

$$\nu_p^* = \frac{1}{2i}\left(1 - \sqrt{\frac{2\bar{\alpha}_s y}{\ln(r'/r)}}\right), \tag{30}$$

which is valid only if $r < r'$. Expanding the argument of the exponential near the saddle point ν_p^* to the second order and integrating gives the double-logarithmic approximation

$$n_p(\mathbf{r}, \mathbf{r}', y)_{\mathrm{DLA}} \approx \frac{r^2}{4\pi^{3/2} r'^4} \frac{(2\bar{\alpha}_s y)^{1/4}}{\ln^{3/4}(r'/r)} e^{2\sqrt{2\bar{\alpha}_s y \ln(r'/r)}}, \quad r < r', \quad \ln(r'/r) \gg \alpha_s y. \tag{31}$$

To derive an analogous expression at $r > r'$ we expand $\chi(\nu)$ near the symmetric pole

$$\chi(\nu)_{\mathrm{DLA}} \approx \frac{1}{1 + 2i\nu}. \tag{32}$$

In analogy to (30) and (31) we derive the saddle point

$$\tilde{\nu}_p^* = \frac{1}{2i}\left(-1 + \sqrt{\frac{2\bar{\alpha}_s y}{\ln(r/r')}}\right), \tag{33}$$

and the dipole density

$$n_p(\mathbf{r}, \mathbf{r}', y)_{\mathrm{DLA}} \approx \frac{1}{4\pi^{3/2} r'^2} \frac{(2\bar{\alpha}_s y)^{1/4}}{\ln^{3/4}(r/r')} e^{2\sqrt{2\bar{\alpha}_s y \ln(r/r')}}, \quad r > r', \quad \ln(r/r') \gg \alpha_s y. \tag{34}$$

B. Dipole evolution in a heavy nucleus

1. Leading twist approximation

Consider the forward elastic dipole-nucleus scattering amplitude $N(\mathbf{r}, \mathbf{b}, Y)$ satisfying the nonlinear evolution

Eq. (11). If the dipole size is much smaller than the saturation scale Q_s, then the quantum evolution of the amplitude is governed by the BFKL equation. Therefore in this case, the general solution is

$$N(\mathbf{r},\mathbf{b},y)_{\mathrm{LT}} = \int_{-\infty}^{\infty} d\nu e^{2\bar{\alpha}_s\chi(\nu)y}(rQ_{s0})^{1+2i\nu}C_\nu^A. \tag{35}$$

The Mellin image C_ν^A of the amplitude $N(\mathbf{r},\mathbf{b},0)_{LT}$ is calculated as follows

$$\begin{aligned} C_\nu^A &= \frac{Q_{s0}}{\pi}\int_0^\infty dr(rQ_{s0})^{-2-2i\nu}N(\mathbf{r},\mathbf{b},0)_{\mathrm{LT}} \\ &= \frac{Q_{s0}}{\pi}\int_0^\infty dr(rQ_{s0})^{-2-2i\nu}\frac{1}{8}r^2Q_{s0}^2 \\ &= \frac{1}{8\pi}\frac{1+(1-2i\nu)\ln\frac{Q_{s0}}{\Lambda}}{(1-2i\nu)^2}. \end{aligned} \tag{36}$$

In the last line of (36) we used the fact that Q_{s0} logarithmically depends on r, see (3) and (4). Analogously to the derivation of (27) we obtain in the leading logarithmic approximation

$$\begin{aligned} N(\mathbf{r},\mathbf{b},y)_{\mathrm{LLA}} &= \frac{rQ_{s0}}{8\pi}\sqrt{\frac{\pi}{14\zeta(3)\bar{\alpha}_s y}}\ln\left(\frac{Q_{s0}}{\Lambda}\right) \\ &\quad\times e^{(\alpha_P-1)y}e^{-(\ln^2(rQ_{s0})/14\zeta(3)\bar{\alpha}_s y)}, \\ \alpha_s y &\gg \ln^2\left(\frac{1}{rQ_{s0}}\right), \end{aligned} \tag{37}$$

where the saddle point is

$$\nu_A^\star = \frac{i\ln(rQ_{s0})}{14\zeta(3)\bar{\alpha}_s y}. \tag{38}$$

In the double-logarithmic approximation (28) the saddle point for the case $r<1/Q_{s0}$ is

$$\nu_A^* = \frac{1}{2i}\left(1-\sqrt{\frac{2\bar{\alpha}_s y}{\ln\frac{1}{rQ_{s0}}}}\right). \tag{39}$$

Repeating the by now familiar procedure we write

$$\begin{aligned} N(\mathbf{r},\mathbf{b},y)_{\mathrm{DLA}} &= \frac{\sqrt{\pi}}{16\pi}\frac{\ln^{1/4}(\frac{1}{rQ_{s0}})}{(2\bar{\alpha}_s y)^{3/4}}r^2Q_{s0}^2\left(1+\sqrt{\frac{2\alpha_s y}{\ln\frac{1}{rQ_{s0}}}}\ln\frac{Q_{s0}}{\Lambda}\right) \\ &\quad\times e^{2\sqrt{2\bar{\alpha}_s y\ln(1/rQ_{s0})}}, \\ r<1/Q_{s0},&\qquad \ln\frac{1}{rQ_{s0}} \gg \alpha_s y. \end{aligned} \tag{40}$$

Next, we consider the case $r>1/Q_s$.

2. Deep saturation region

The solution to the BK Eq. (11) deeply in the saturation regime was found in [71–73]. With the logarithmic accuracy the dominant dipole splitting corresponds to the configuration in which the size of one of the daughter dipoles ($\sim 1/Q_s$) is much smaller than the other (see Sec. VI). Denote again $\mathbf{r}=\mathbf{x}-\mathbf{y}$ and $\mathbf{w}=\mathbf{z}-\mathbf{y}$. In the saturation region we have either $w \ll r \approx |\mathbf{w}-\mathbf{r}|$ or the symmetric configuration $|\mathbf{w}-\mathbf{r}| \ll r \approx w$. Both give equal contribution to the integral over $\mathbf{w}$. Restricting ourself to the case $w \ll r$ and doubling the integral we write the BK equation as follows:

$$\begin{aligned} \frac{\partial N(\mathbf{r},\mathbf{b},y)}{\partial y} &\approx \frac{\alpha_s C_F}{\pi}2\int_{1/Q_s^2}^{r^2}\frac{dw^2}{w^2}[N(\mathbf{w},\mathbf{b},y) \\ &\quad - N(\mathbf{w},\mathbf{b},y)N(\mathbf{r},\mathbf{b},y)]. \end{aligned} \tag{41}$$

Now, for the reason that in the saturation region, the amplitude $N(\mathbf{r},\mathbf{b},y)$ is close to unity we render (41) as

$$\begin{aligned} -\frac{\partial\{1-N(\mathbf{r},\mathbf{b},y)\}}{\partial y} &\approx \frac{\alpha_s C_F}{\pi}2\int_{1/Q_s^2}^{r^2}\frac{dw^2}{w^2}\{1-N(\mathbf{r},\mathbf{b},y)\} \\ &= \frac{2\alpha_s C_F}{\pi}\ln(r^2Q_s^2)\{1-N(\mathbf{r},\mathbf{b},y)\}. \end{aligned} \tag{42}$$

The saturation scale $Q_s(y)$ can be found by equating the argument of the exponent in (40) to a constant which yields [71,74]

$$Q_s(y) \approx Q_{s0}e^{2\bar{\alpha}_s y}. \tag{43}$$

Introducing a new scaling variable $\tau=\ln(r^2Q_s^2)$ we solve (42) and find the high energy limit of the forward scattering amplitude (in the fixed coupling approximation). It reads [71]

$$N(\mathbf{r},\mathbf{b},y) = 1-S_0e^{-\tau^2/8} = 1-S_0e^{-(1/8)\ln^2(r^2Q_s^2)}, \tag{44}$$

where we approximated $C_F \approx N_c/2$ in the large N_c limit. S_0 is the integration constant. It determines the value of the amplitude at the critical line $r(y)=1/Q_s(y)$.

V. DIFFRACTIVE CROSS SECTION IN THE QUASICLASSICAL APPROXIMATION

Careful inspection of (1) reveals that the cross section vanishes when the size of the onium $\mathbf{r}=\mathbf{x}-\mathbf{y}$ is much larger than the characteristic scale $1/Q_{s0}$. This is in a sharp contrast with the inclusive gluon production case [26] where the cross section stays finite at $r\to\infty$. To understand the reason for such different behavior, consider a sample diagrams contributing to each of the processes shown in Fig. 4. In diagram 4(a), corresponding to the inclusive case, the propagator of the $q\bar{q}g$ system in the nucleus is proportional to $e^{-(1/4)(\mathbf{x}-\mathbf{z}_1)^2Q_{s0}^2}$ while the gluon emission amplitude is proportional to $\frac{g(\mathbf{x}-\mathbf{z}_1)}{|\mathbf{x}-\mathbf{z}_1|^2}$. Both do not involve the $\mathbf{y}$ coordinate at all and are finite at $\mathbf{y}\to\infty$. On the contrary, in diagram 4(b), corresponding to the diffractive case, the propagator involves both $\mathbf{x}$ and $\mathbf{y}$ coordinates, see (2), no factorization of $\mathbf{y}$ dependence similar to the inclusive case happens. All other diagrams contributing to these two processes can be analyzed in the same way. Let

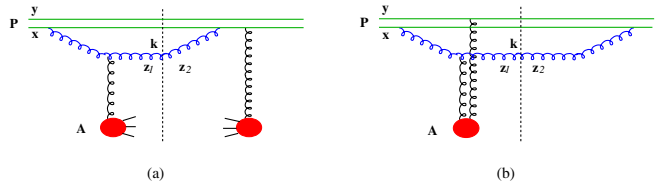

FIG. 4 (color online). An example of diagrams contributing to (a) inclusive gluon production and (b) diffractive gluon production.

us look at the color structure of the $q\bar{q}g$ system in the two cases. By the Pomeranchuk theorem, the exchanged (Coulomb) gluons are in the color singlet state. Therefore, we notice that in diagram 4(a) the $q\bar{q}g$ system is in the color octet state and its propagator through the nucleus equals the propagator of a gluon dipole, whereas in diagram 4(b) the $q\bar{q}g$ system is always in the color singlet state corresponding to the quark dipole. This feature can be seen also in expressions for the propagator, one involving the gluon saturation scale Q_{s0}^2 (inclusive case), another involving the quark saturation scale $\frac{C_F}{N_c} Q_{s0}^2 \approx \frac{1}{2} Q_{s0}^2$ (diffractive case).

Now we would like to determine how does the diffractive cross section behave in the quasiclassical approximation. Consider the following integral appearing in the right-hand side (r.h.s.) of (7) and (15):

$$J(\mathbf{r}, y) = \frac{1}{\pi} \int d^2w \frac{\mathbf{r}^2}{(\mathbf{w}-\mathbf{r})^2 \mathbf{w}^2} [N(\mathbf{r}, \mathbf{b}, y) - N(\mathbf{w}-\mathbf{r}, \mathbf{b}, y) - N(\mathbf{w}, \mathbf{b}, y) + N(\mathbf{w}-\mathbf{r}, \mathbf{b}, y) N(\mathbf{w}, \mathbf{b}, y)]^2. \quad (45)$$

Let us analyze its behavior in the quasiclassical case ($y = 0$) for small $r < 1/Q_{s0}$ and large $r > 1/Q_{s0}$ onium sizes.

A. Dilute regime $r < 1/Q_{s0}$

In the case of small onium we divide the entire integral over $\mathbf{w}$ into three terms as follows:

$$J(\mathbf{r}, 0) \approx \int_0^r \frac{dw^2}{w^2} [1 - N(\mathbf{r}, \mathbf{b}, 0)]^2 N^2(\mathbf{w}, \mathbf{b}, 0) + r^2 \int_r^{1/Q_{s0}} \frac{dw^2}{w^4} [N(\mathbf{r}, \mathbf{b}, 0) - 2N(\mathbf{w}, \mathbf{b}, 0) + N^2(\mathbf{w}, \mathbf{b}, 0)]^2 + r^2 \int_{1/Q_{s0}}^{\infty} \frac{dw^2}{w^4} [N(\mathbf{r}, \mathbf{b}, 0) - 2N(\mathbf{w}, \mathbf{b}, 0) + N^2(\mathbf{w}, \mathbf{b}, 0)]^2, \quad (46)$$

where (46) holds in logarithmic approximation. We can estimate each term utilizing the fact that according to (5)

$$N(\mathbf{r}, \mathbf{b}, 0) \approx \begin{cases} 1, & r \gg 1/Q_{s0}, \\ \frac{1}{8} r^2 Q_{s0}^2, & r \ll 1/Q_{s0}. \end{cases} \quad (47)$$

Moreover, in the last two terms in (47) $N(\mathbf{r}, \mathbf{b}, 0)$ can be neglected since in most of the integration regions $w \gg r$. Indeed, in the second term in the r.h.s. of (46) it can be seen once we neglect $N^2(\mathbf{w}, \mathbf{b}, 0)$ and expand $N(\mathbf{w}, \mathbf{b}, 0)$ at small w. In the third term in the r.h.s. of (46) we have $2N(\mathbf{w}, \mathbf{b}, 0) - N^2(\mathbf{w}, \mathbf{b}, 0) \approx 1$ while $N(\mathbf{r}, \mathbf{b}, 0) \ll 1$. Accordingly, expanding the integrands using (47) we find that the first term in the r.h.s. of (46) is of the order $\mathcal{O}(r^8 Q_{s0}^8)$, whereas the second and the third ones are of the order $\mathcal{O}(r^2 Q_{s0}^2)$. Therefore, the last two terms in (46) dominate in the regime $rQ_{s0} \ll 1$. It is customary to denote

$$N_G(\mathbf{r}, \mathbf{b}, y) = 2N(\mathbf{r}, \mathbf{b}, y) - N^2(\mathbf{r}, \mathbf{b}, y), \quad (48)$$

which has the meaning of the *gluon dipole* forward elastic scattering amplitude. In terms of this quantity the function $J(\mathbf{r}, 0)$ reads

$$J(\mathbf{r}, 0) \approx r^2 \int_0^{\infty} \frac{dw^2}{w^4} N_G^2(\mathbf{w}, \mathbf{b}, 0), \qquad r \ll 1/Q_{s0}, \quad (49)$$

where the lower limit of integration (r) has been set to zero with logarithmic accuracy (note that the second integral in the r.h.s. of (46) is dominated by dipoles of size $w \sim 1/Q_{s0} \gg r$).

It is useful to notice, that (49) holds also in the case the low-x evolution is taken into account. In the quasiclassical approximation the integral (49) can be done if we treat Q_{s0} as a w-independent constant neglecting its logarithmic variation. In that case, substituting (5) we derive

$$J(\mathbf{r}, 0) \approx \frac{1}{4} \ln 2 r^2 Q_{s0}^2, \qquad r \ll 1/Q_{s0}, \quad (50)$$

The cross section is obtained using (7) and (45). We have

$$\frac{d\sigma}{dy} = \frac{\alpha_s C_F}{\pi} S_A J(r, 0) = \frac{\alpha_s C_F \ln 2}{4\pi} S_A r^2 Q_{s0}^2, \qquad r \ll 1/Q_{s0}. \quad (51)$$

B. Dense regime $r > 1/Q_{s0}$

As in the previous case we divide the integral into three parts

$$J(\mathbf{r}, 0) \approx \int_0^{1/Q_{s0}} \frac{dw^2}{w^2} [1 - N(\mathbf{r}, \mathbf{b}, 0)]^2 N^2(\mathbf{w}, \mathbf{b}, 0) \times \int_{1/Q_{s0}}^{r} \frac{dw^2}{w^2} [1 - N(\mathbf{r}, \mathbf{b}, 0)]^2 N^2(\mathbf{w}, \mathbf{b}, 0) + r^2 \int_r^{\infty} \frac{dw^2}{w^4} [N(\mathbf{r}, \mathbf{b}, 0) - 2N(\mathbf{w}, \mathbf{b}, 0) + N^2(\mathbf{w}, \mathbf{b}, 0)]^2. \quad (52)$$

Utilizing (47) we simplify (52) in the logarithmic approximation as follows

$$J(\mathbf{r}, 0) \approx [N(\mathbf{r}, \mathbf{b}, 0) - 1]^2 \left(\int_0^{1/Q_{s0}} \frac{dw^2}{w^2} \frac{1}{64} w^4 Q_{s0}^4 + \int_{1/Q_{s0}}^{r} \frac{dw^2}{w^2} + r^2 \int_r^{\infty} \frac{dw^2}{w^4} \right). \quad (53)$$

$$\approx [N(\mathbf{r}, \mathbf{b}, 0) - 1]^2 \ln(r^2 Q_{s0}^2), \qquad r \gg 1/Q_{s0}. \tag{54}$$

Going from (53) to (54) we kept only the second term in the brackets in (53) as it is logarithmically enhanced. Formula (54) is valid in the case of low-x evolution as well. Substituting (5) into (54) yields

$$J(r) = \ln(r^2 Q_{s0}^2) e^{-(1/4) r^2 Q_{s0}^2}, \qquad r \gg 1/Q_{s0}. \tag{55}$$

Finally, the cross section follows from (7), (45), and (55) as

$$\frac{d\sigma}{dy} = \frac{\alpha_s C_F}{\pi} S_A \ln(r^2 Q_{s0}^2) e^{-(1/4) r^2 Q_{s0}^2}, \qquad r \gg 1/Q_{s0}. \tag{56}$$

The striking feature of this formula is strong exponential suppression of diffractive gluon production for large onium. We will see in the next section that this result completely changes when the quantum evolution in the onium becomes an important effect.

VI. DIFFRACTIVE CROSS SECTION INCLUDING LOW-x EVOLUTION

Using (15) and (45) we write

$$\frac{d\sigma}{dy} = \frac{\alpha_s C_F}{\pi} S_A \int d^2 r' n_p(\mathbf{r}, \mathbf{r}', Y - y) J(\mathbf{r}', y). \tag{57}$$

A. Dilute regime $r < 1/Q_s(y)$

As in the quasiclassical case, first we are going to find the kinematic region which gives the largest (logarithmic) contribution to the integral. We have

$$\frac{d\sigma}{dy} = \frac{\alpha_s C_F}{\pi} S_A 2\pi \Bigg[\int_0^r dr' r' n_p(\mathbf{r}, \mathbf{r}', Y - y) J(\mathbf{r}', y) + \int_r^{1/Q_s} dr' r' n_p(\mathbf{r}, \mathbf{r}', Y - y) J(\mathbf{r}', y) + \int_{1/Q_s}^{\infty} dr' r' n_p(\mathbf{r}, \mathbf{r}', Y - y) J(\mathbf{r}', y) \Bigg]. \tag{58}$$

As has been noted in the previous sections, Eqs. (49) and (54) hold also in the evolution case, provided the y dependence is explicitly indicated in the arguments of $J(\mathbf{r}, y)$ and $N(\mathbf{r}, \mathbf{b}, y)$. Generalization of (50) reads

$$J(\mathbf{r}', y) \approx C_0 r'^2 Q_s^2(y), \qquad r' \ll 1/Q_s(y), \tag{59}$$

where C_0 is a constant which depends on a particular functional form of $N_G(\mathbf{r}, \mathbf{b}, y)$ and can be found numerically from (11). Using (44) in (54) gives another limit of function $J(\mathbf{r}', y)$

$$J(\mathbf{r}', y) \approx S_0^2 e^{-\ln^2(r' Q_s)} \ln(r'^2 Q_s^2), \qquad r' \gg 1/Q_s(y). \tag{60}$$

Accordingly, using (31) or (34) depending on the relation between r and r', i. e., $n_p \sim r^2/r'^4$ if $r < r'$ or $n_p \sim 1/r'^2$ if $r > r'$, as well as (59) and (60), we estimate that the second integral in (58) is enhanced by $\ln\frac{1}{rQ_s}$ with respect to the first one, whereas the third integral is vanishingly small. Thus,

$$\frac{d\sigma}{dy} \approx \frac{\alpha_s C_F}{\pi} S_A 2\pi \int_r^{1/Q_s} dr' r' n_p(\mathbf{r}, \mathbf{r}', Y - y) J(\mathbf{r}', y) = \frac{2 C_0 \alpha_s C_F S_A}{4\pi^{3/2}} r^2 Q_s^2 \int_r^{1/Q_s} \frac{dr'}{r'} \frac{(2\bar{\alpha}_s (Y - y))^{1/4}}{\ln^{3/4} \frac{r'}{r}} \times e^{2\sqrt{2\bar{\alpha}_s (Y-y) \ln(r'/r)}}. \tag{61}$$

Changing to a new integration variable η defined as $\eta^2 = \ln\frac{r'}{r}$ the integral in (61) can be taken explicitly in terms of the imaginary error function. In the double-logarithmic approximation the result reads

$$\frac{d\sigma}{dy} = \frac{C_0 \alpha_s C_F S_A}{4\pi^{3/2}} \frac{r^2 Q_s^2}{(2\bar{\alpha}_s (Y - y) \ln\frac{1}{rQ_s})^{1/4}} e^{2\sqrt{2\bar{\alpha}_s (Y-y) \ln(1/rQ_s)}}, \qquad r \ll 1/Q_s(y). \tag{62}$$

Both the quasiclassical result (51) and its quantum counterpart (62) show that the cross section is proportional to r^2 as required by the color transparency.

B. Dense regime $r > 1/Q_s$

Analogously to (58) we get

$$\frac{d\sigma}{dy} = \frac{\alpha_s C_F}{\pi} S_A 2\pi \Bigg[\int_0^{1/Q_s} dr' r' n_p(\mathbf{r}, \mathbf{r}', Y - y) J(\mathbf{r}', y) + \int_{1/Q_s}^{r} dr' r' n_p(\mathbf{r}, \mathbf{r}', Y - y) J(\mathbf{r}', y) + \int_r^{\infty} dr' r' n_p(\mathbf{r}, \mathbf{r}', Y - y) J(\mathbf{r}', y) \Bigg]. \tag{63}$$

The logarithmically enhanced contribution arises from the second integral which—upon substitution of (60) and (34)—becomes

$$\frac{d\sigma}{dy} = \frac{\alpha_s C_F S_A}{2\pi^{3/2}} S_0^2 (2\bar{\alpha}_s (Y - y))^{1/4} \int_{1/Q_s}^{r} \frac{dr'}{r'} \times \frac{\ln(r'^2 Q_s^2)}{\ln^{3/4} \frac{r}{r'}} e^{-\ln(r' Q_s)} e^{2\sqrt{2\bar{\alpha}_s (Y-y) \ln(r/r')}}. \tag{64}$$

Note that in the relevant kinematic region $1/Q_s \ll r' \ll r$ we can approximate $\ln\frac{r}{r'} = \ln(rQ_s) + \ln\frac{1}{r'Q_s} \approx \ln(rQ_s)$. The integral over r' then becomes trivial yielding the final result

$$\frac{d\sigma}{dy} = \frac{\alpha_s C_F S_A}{2\pi^{3/2}} S_0^2 \frac{(2\bar{\alpha}_s (Y - y))^{1/4}}{\ln^{3/4}(rQ_s)} e^{2\sqrt{2\bar{\alpha}_s (Y-y) \ln(rQ_s)}}, \qquad r \gg 1/Q_s(y). \tag{65}$$

We observe that the cross section given by (65) is an *increasing* function of the rapidity interval $Y - y$ between the onium and the nucleus. Together with the quasiclassical

expression (56) it implies that the total cross section for the diffractive gluon production in a scattering of a large onium off the heavy nucleus is nonvanishing only if the low-x evolution in onium is an important effect. This can be seen directly in Fig. 2: the gluon multiplicity arises from the cut Pomeron attached to the onium. This observation has important phenomenological consequences as we discuss in the next section.

VII. DISCUSSION AND SUMMARY

In this paper we discussed the coherent diffractive gluon production in high energy onium-nucleus collisions. The gluon multiplicity in the case of onium of small size $r < 1/Q_s$ is given by (51) and (62) and can be summarized as follows

$$\frac{dN_D(y)}{dy} \propto r^2 Q_s^2(y) xG(\exp(y-Y), Q_s^2), \qquad r \ll Q_s, \tag{66}$$

where $xG(x, Q^2)$ is a gluon distribution function at momentum scale Q^2. Gluon multiplicity vanishes in the limit $r \to 0$ as is required by the color transparency.

In the other limit of large onium, the gluon production cross section vanishes in the quasiclassical approximation as implied by (56). At $\bar{\alpha}_s(Y-y) \gtrsim 1$ the evolution effects in onium play an increasingly important role. It is the cut Pomeron, connecting the onium and the dipole ($\mathbf{r}'$) emitting the triggered gluon, which contributes to the fast increase in gluon multiplicity as interval $Y-y$ increases. One way to see it is to recall that during the linear evolution dipoles of various sizes are produced from the parent onium of size r. We explained in (63) and (64) that the main contribution to the multiplicity stems from the dipoles of size $r' \sim 1/Q_s$ no matter how big the initial dipole r is. The resulting expression (65) has the following behavior

$$\frac{dN_D(y)}{dy} \propto xG(\exp(y-Y), Q_s^2), \qquad r \gg Q_s, \quad (Y-y) \gtrsim 1/\alpha_s. \tag{67}$$

Dependence of the diffractive gluon multiplicity on the onium size is summarized in Fig. 5.

To the extent that the large onium can serve as a model for proton, (56) and (65) describe the diffractive gluon production in proton-nucleus collisions. As such it has a direct implications to the RHIC and LHC phenomenology. Phenomenological studies show that the gluon saturation at RHIC starts to impact the gluon and valence quark spectra at rapidities $\eta \simeq 1$ (and larger). In our notations it corresponds to the rapidity interval $y \simeq 6$ between the gluon and the heavy nucleus and $Y - y \simeq 4$ between the proton and the gluon. This corresponds to $x_p \simeq e^{-4} \approx 0.02$ which is perhaps insufficient to have a sizable low-x effect in proton implying a very low multiplicity of diffractive gluon production. On the other hand, exploring the backward rapidity region $\eta < 0$ will not allow one to probe the gluon saturation in the nucleus. Therefore, if the typical interquark distance in proton is larger than $\sim 1/Q_s \simeq 0.2$ fm, then we do not expect a significant multiplicity of gluons in *coherent* diffraction of a proton on nucleus at RHIC, see Fig. 5.[1]

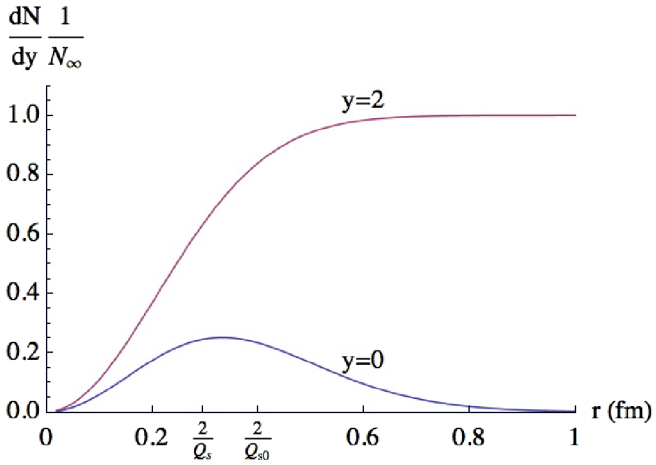

FIG. 5 (color online). Relative multiplicity of diffractive gluons as a function of the onium size r in the quasiclassical approximation (labeled $y = 0$) and at very low x ($y = 2$). The rapidity values correspond to those at RHIC as explained in the text. We chose $Q_{s0} = 1$ GeV and $Q_s = 1.35$ GeV. N_∞ is a normalization constant.

The situation radically changes at LHC where an additional rapidity window $\Delta\eta \simeq 6$ opens up. From the point of view of gluon saturation, the midrapidity in pA at LHC is expected to be similar to the rapidity $\eta = 3$ at RHIC [32,40]. At the same time, at the LHC midrapidity, $x_p \simeq e^{-7} = 0.001$ which is certainly sufficient for the low-x evolution to take place in proton. Therefore, we expect that measurements of the diffractive gluon production in pA collisions at LHC will be a sensitive probe of the low-x dynamics. At EIC the typical dipole size r is determined by the photon virtuality Q as $r \sim 1/Q$ which makes it possible the detailed study gluon saturation using the diffractive gluon production in different kinematical regions (see, e.g., [75,76]).

An interesting extension of our work is a case of diffractive production with small rapidity gap $Y_0 < y$, which will be relevant at LHC. Of special interest is dependence of the differential cross section for diffractive gluon production on transverse momentum of produced gluon. We

[1]Clearly, this conclusion does not hold if proton's valence quarks form a diquark-quark configuration where the diquark has small size. From this perspective the diffractive gluon production at RHIC is a sensitive probe of the valence quark configuration in proton.

are addressing this and other issues in the forthcoming publication.

ACKNOWLEDGMENTS

K. T. is grateful to Yuri Kovchegov, Genya Levin, and Jianwei Qiu for very informative and helpful discussions. The work of K. T. was supported in part by the U.S. Department of Energy under Grant No. DE-FG02-87ER40371. He would like to thank RIKEN, BNL, and the U.S. Department of Energy (Contract No. DE-AC02-98CH10886) for providing facilities essential for the completion of this work.

[1] L. D. McLerran and R. Venugopalan, Phys. Rev. D **49**, 2233 (1994); Phys. Rev. D **49**, 3352 (1994); Phys. Rev. D **50**, 2225 (1994).
[2] J. Jalilian-Marian, A. Kovner, A. Leonidov, and H. Weigert, Nucl. Phys. **B504**, 415 (1997).
[3] J. Jalilian-Marian, A. Kovner, A. Leonidov, and H. Weigert, Phys. Rev. D **59**, 014014 (1998).
[4] J. Jalilian-Marian, A. Kovner, A. Leonidov, and H. Weigert, Phys. Rev. D **59**, 034007 (1999); **59**, 099903 (1999).
[5] J. Jalilian-Marian, A. Kovner, and H. Weigert, Phys. Rev. D **59**, 014015 (1998).
[6] A. Kovner, J. G. Milhano, and H. Weigert, Phys. Rev. D **62**, 114005 (2000); H. Weigert, Nucl. Phys. **A703**, 823 (2002).
[7] E. Iancu, A. Leonidov, and L. D. McLerran, Nucl. Phys. **A692**, 583 (2001).
[8] E. Iancu, A. Leonidov, and L. D. McLerran, Phys. Lett. B **510**, 133 (2001).
[9] E. Iancu and L. D. McLerran, Phys. Lett. B **510**, 145 (2001).
[10] E. Ferreiro, E. Iancu, A. Leonidov, and L. McLerran, Nucl. Phys. **A703**, 489 (2002).
[11] L. V. Gribov, E. M. Levin, and M. G. Ryskin, Phys. Rep. **100**, 1 (1983).
[12] A. H. Mueller and J. w. Qiu, Nucl. Phys. **B268**, 427 (1986).
[13] K. J. Golec-Biernat and M. Wusthoff, Phys. Rev. D **59**, 014017 (1998).
[14] K. J. Golec-Biernat and M. Wusthoff, Phys. Rev. D **60**, 114023 (1999).
[15] E. Gotsman, E. Levin, M. Lublinsky, U. Maor, and K. Tuchin, Phys. Lett. B **492**, 47 (2000).
[16] E. Gotsman, E. Levin, M. Lublinsky, U. Maor, and K. Tuchin, arXiv:hep-ph/0007261.
[17] E. Gotsman, E. Levin, M. Lublinsky, U. Maor, and K. Tuchin, Nucl. Phys. **A697**, 521 (2002).
[18] Y. V. Kovchegov and L. D. McLerran, Phys. Rev. D **60**, 054025 (1999); **62**, 019901 (2000).
[19] E. Levin and M. Lublinsky, Nucl. Phys. **A712**, 95 (2002).
[20] E. Levin and M. Lublinsky, Eur. Phys. J. C **22**, 647 (2002).
[21] J. Bartels, K. J. Golec-Biernat, and H. Kowalski, Phys. Rev. D **66**, 014001 (2002).
[22] D. Kharzeev and M. Nardi, Phys. Lett. B **507**, 121 (2001).
[23] D. Kharzeev and E. Levin, Phys. Lett. B **523**, 79 (2001).
[24] D. Kharzeev, E. Levin, and M. Nardi, Phys. Rev. C **71**, 054903 (2005).
[25] D. Kharzeev, E. Levin, and M. Nardi, Nucl. Phys. **A730**, 448 (2004); **A743**, 329 (2004).
[26] Y. V. Kovchegov and A. H. Mueller, Nucl. Phys. **B529**, 451 (1998).
[27] Y. V. Kovchegov and K. Tuchin, Phys. Rev. D **65**, 074026 (2002).
[28] M. A. Braun, Phys. Lett. B **483**, 105 (2000).
[29] A. Dumitru and L. D. McLerran, Nucl. Phys. **A700**, 492 (2002).
[30] J. P. Blaizot, F. Gelis, and R. Venugopalan, Nucl. Phys. **A743**, 13 (2004).
[31] D. Kharzeev, E. Levin, and L. McLerran, Phys. Lett. B **561**, 93 (2003).
[32] D. Kharzeev, Y. V. Kovchegov, and K. Tuchin, Phys. Rev. D **68**, 094013 (2003).
[33] D. Kharzeev, Y. V. Kovchegov, and K. Tuchin, Phys. Lett. B **599**, 23 (2004).
[34] R. Baier, A. Kovner, and U. A. Wiedemann, Phys. Rev. D **68**, 054009 (2003).
[35] E. Iancu, K. Itakura, and D. N. Triantafyllopoulos, Nucl. Phys. **A742**, 182 (2004).
[36] F. Gelis and R. Venugopalan, Phys. Rev. D **69**, 014019 (2004).
[37] K. Tuchin, Phys. Lett. B **593**, 66 (2004).
[38] J. P. Blaizot, F. Gelis, and R. Venugopalan, Nucl. Phys. **A743**, 57 (2004).
[39] Y. V. Kovchegov and K. Tuchin, Phys. Rev. D **74**, 054014 (2006).
[40] K. Tuchin, Nucl. Phys. **A798**, 61 (2008).
[41] D. Kharzeev and K. Tuchin, Nucl. Phys. **A735**, 248 (2004).
[42] D. Kharzeev and K. Tuchin, Nucl. Phys. **A770**, 40 (2006).
[43] F. Gelis and A. Peshier, Nucl. Phys. **A697**, 879 (2002).
[44] A. Dumitru and J. Jalilian-Marian, Phys. Rev. Lett. **89**, 022301 (2002).
[45] J. Jalilian-Marian, Nucl. Phys. **A753**, 307 (2005).
[46] R. Baier, A. H. Mueller, and D. Schiff, Nucl. Phys. **A741**, 358 (2004).
[47] J. Jalilian-Marian, Nucl. Phys. **A739**, 319 (2004).
[48] M. A. Betemps and M. B. Gay Ducati, Phys. Rev. D **70**, 116005 (2004); Phys. Lett. B **636**, 46 (2006).
[49] Y. Li and K. Tuchin, Phys. Rev. D **75**, 074022 (2007).
[50] K. Tuchin, Nucl. Phys. **A783**, 173 (2007).
[51] J. Jalilian-Marian and Y. V. Kovchegov, Prog. Part. Nucl. Phys. **56**, 104 (2006).
[52] M. Wusthoff, Phys. Rev. D **56**, 4311 (1997).
[53] J. Bartels, H. Jung, and M. Wusthoff, Eur. Phys. J. C **11**, 111 (1999).
[54] B. Z. Kopeliovich, A. Schafer, and A. V. Tarasov, Phys. Rev. D **62**, 054022 (2000).

[55] Y. V. Kovchegov, Phys. Rev. D **64**, 114016 (2001); **68**, 039901 (2003).
[56] K. J. Golec-Biernat and C. Marquet, Phys. Rev. D **71**, 114005 (2005).
[57] C. Marquet, Nucl. Phys. **B705**, 319 (2005).
[58] C. Marquet, Phys. Rev. D **76**, 094017 (2007).
[59] S. Munier and A. Shoshi, Phys. Rev. D **69**, 074022 (2004).
[60] A. Kovner, M. Lublinsky, and H. Weigert, Phys. Rev. D **74**, 114023 (2006).
[61] A. Kovner and U. A. Wiedemann, Phys. Rev. D **64**, 114002 (2001).
[62] B. Z. Kopeliovich, A. V. Tarasov, and A. Schafer, Phys. Rev. C **59**, 1609 (1999).
[63] A. H. Mueller, Nucl. Phys. **B415**, 373 (1994); A. H. Mueller and B. Patel, Nucl. Phys. **B425**, 471 (1994); A. H. Mueller, Nucl. Phys. **B437**, 107 (1995).
[64] A. H. Mueller, Nucl. Phys. **B335**, 115 (1990).
[65] V. A. Abramovsky, V. N. Gribov, and O. V. Kancheli, Yad. Fiz. **18**, 595 (1973) [Sov. J. Nucl. Phys. **18**, 308 (1974)].
[66] E. A. Kuraev, L. N. Lipatov, and V. S. Fadin, Zh. Eksp. Teor. Fiz. **72**, 377 (1977) [Sov. Phys. JETP **45**, 199 (1977)].
[67] I. I. Balitsky and L. N. Lipatov, Yad. Fiz. **28**, 1597 (1978) [Sov. J. Nucl. Phys. **28**, 822 (1978)].
[68] I. Balitsky, Nucl. Phys. **B463**, 99 (1996).
[69] Y. V. Kovchegov, Phys. Rev. D **60**, 034008 (1999).
[70] Y. V. Kovchegov and E. Levin, Nucl. Phys. **B577**, 221 (2000).
[71] E. Levin and K. Tuchin, Nucl. Phys. **B573**, 833 (2000).
[72] E. Levin and K. Tuchin, Nucl. Phys. **A691**, 779 (2001).
[73] E. Levin and K. Tuchin, Nucl. Phys. **A693**, 787 (2001).
[74] J. Bartels and E. Levin, Nucl. Phys. **B387**, 617 (1992).
[75] E. Gotsman, E. Levin, U. Maor, L. D. McLerran, and K. Tuchin, Phys. Lett. B **506**, 289 (2001).
[76] E. Gotsman, E. Levin, U. Maor, L. D. McLerran, and K. Tuchin, Nucl. Phys. **A683**, 383 (2001).